Vibration Modes and Sound Characteristic Analysis for Different Sizes of Singing Bowls

Bor-Tsuen Wang [1,*], *Chun-Lang Tsai* [1] , and *Ying-Hui Wu* [2]

[1]Department of Mechanical Engineering, National Pingtung University of Science and Technology, Pingtung, 912, Taiwan
[2]Machinery Division, National Nei-Pu Senior Agricultural Industrial Vocational School, Pingtung, 912, Taiwan

Abstract. The singing bowl is used not only for the instrument of Buddhism but also for musical therapy. This work aims to investigate the correlation of vibration modes and percussion sound for singing bowls. A typical singing bowl is first selected to perform finite element analysis (FEA) for theoretical modal analysis (TMA) as well as experimental modal analysis (EMA). Modal parameters of singing bowl, including natural frequencies and mode shapes, can be obtained from analysis and experiment, respectively. Singing bowl FE model can then be updated and verified by adjusting material properties and used to predict structural vibration modes. The percussion sound of singing bowl is also measured to obtain its sound spectrum. The peak frequency response of singing bowl sound can be interpreted and contributed from circular vibration modes of the bowl. With the knowledge of sound generation mechanism for the singing bowl, this work also studies the percussion sound characteristics of seven different sizes of singing bowls. Results show the fundamental frequency and overtone frequencies of singing bowl percussion sound are higher for the smaller size. Interestingly, that the peak resonant frequencies have near the integer ratio relationship makes the singing bowl revealing harmony sound effects. The radiated sound spectrum can be well calibrated and predicted for different sizes of singing bowls. This work shows the analytical and experimental approaches in studying the singing bowl percussion sound that strongly correlated to structural vibration modes and can be adopted for future development of singing bowls.

1 Introduction

Singing bowls also known as Tibetan singing bowls from Himalayan can produce harmony sound. Singing bowls are not only used for the instrument of Buddhism but also for musical therapy. This work aims to investigate the vibration characteristics of a singing bowl by finite element analysis (FEA) and experimental modal analysis (EMA).

Wang *et al.* [1] presented structural and vibro-acoustic analysis on the harmonic sound plate made by steel which vibration modes and acoustic sound pressure modes can be

---

[*] Corresponding author: wangbt@mail.npust.edu.tw

identified and related to the percussion sound. Wang *et al.* [2] further explored the possibility of using glass material to manufacture the harmonic glass plate (HGP). With the use of FEA for design aid and EMA for the verification, the design of HGP can be achieved from the steel to the glass. The numerical analysis and experimental techniques are crucial for obtaining structural vibration modes as well as sound characteristics.

Bells are similar to singing bowls and have drawn much attention in scientific study. Pan [3] examined the ancient Chinese musical bell which is the almond-shape cross section rather than circular bell. The almond-shape bell can produce two-tone effect for structural vibration mode properties. Lee *et al.* [4] investigated the correlation between percussion sound and vibration modes of Korean bell. With the aid of FEA, they analysed bell's vibration mode shapes and predicted the percussion sound. The optimum percussion location can be designed to obtain the lasting longer sound. McLachlan *et al.* [5] adopted FEA to design the bell that can generate harmonic sound. The geometry of bell was optimized to obtain the special sound quality of bell. McLachlan [6] indicated the major parameters affecting the bell's percussion sound are the thickness, height, radius, and curvature shape and cone angle of bell. Fletcher *et al.* [7] measured the sound spectrum for different bells applied with different levels of impact forces. The percussion sound responses are shown with different decay effects.

Different musical instruments with different sound generation mechanisms are of interest. Myers *et al.* [8] showed the sound generation mechanism for brass instrument. Different geometry variation and effects on radiated sound frequencies were investigated. For guitars, other than the string vibration the radiated sound is amplified through the resonance body with sound hole. Ezcurra [9] applied FEA to calibrate the material properties of sound board and examined vibration mode shapes of sound board to observe the generated sound spectrum. Boullosa [10] conducted sound and vibration measurement on several guitars to compare the radiated sound characteristics.

Wang *et al.* [11] presented correlation study on a singing bowl between vibration modes and percussion sound spectrum. The ring vibration modes can be known dominating the percussion sound response, and different striking methods may result in a slight different sound effect. This work aims to study a series of seven singing bowls from the large size to small ones. Theoretical modal analysis (TMA) on a typical singing bowl is first performed by FEA. EMA on the singing bowl is also carried out to verify vibration modes, including natural frequencies and mode shapes. The percussion sound spectrum can then be measured and interpreted by vibration modes of the singing bowl. Finally, the sound spectrums for the seven different sizes of singing bowls are studied to calibrate the differences, such as the fundamental frequency and overtone frequencies.

2 Analyses and Verification of Singing Bowl Vibration Modes

Fig. 1 shows the typical singing bowl A with the height of 128mm and the radius of 260mm. Both FEA and EMA will be performed, respectively, on the singing bowl A to obtain its natural frequencies and corresponding mode shapes. Fig. 2 shows the procedure for model verification (MV). The purpose of MV is to calibrate the finite element (FE) model of singing bowl that can be equivalent to the real structure.
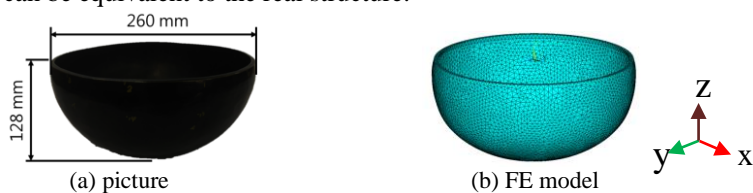

(a) picture   (b) FE model
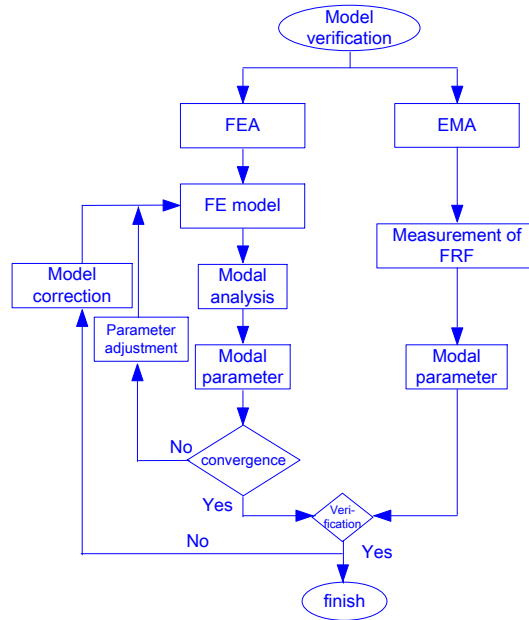
Fig. 1. Typical singing bowl A.

Fig. 2. Procedures for model verification (MV) .

The first step in MV is to perform FEA on the singing bowl. The FE model for the singing bowl as shown in Fig. 1(b) is built and performed TMA to numerically obtain structural modal parameters, including natural frequencies and mode shapes. The singing bowl FE model is constructed by 8-node brick elements (SOLID187) in ANSYS. The singing bowl is made of copper alloy, which material properties are density 4802.6 kg/m^3, Young's modulus 39.37 GPa and Poisson ratio 0.3. The material properties are calibrated after MV. Table 1 shows the convergence analysis of singing bowl FE models. Model (D) with 26,348 elements and 53,226 nodes is adequate for reasonable and accurate analysis in comparison of errors of natural frequencies between Models (D) and (C), within 0.2% up to 2000 Hz.

Table 1. Convergence analysis of singing bowl FE models

	Model (A)	Model (B)	Model (C)	Model (D)	% B vs. A	% C vs. B	% C vs. D
elements	6,689	10,131	18,399	26,348	-	-	-
nodes	13,637	20,595	37,217	53,226	-	-	-
F-07 (Hz)	132.0	130.9	130.2	130.1	0.84	0.54	0.08
F-09 (Hz)	369.9	366.4	364.2	363.8	0.96	0.60	0.11
F-11 (Hz)	699.2	692.3	687.2	686.3	1.00	0.74	0.13
F-13 (Hz)	1107.4	1095.7	1086.5	1084.8	1.07	0.85	0.16
F-15 (Hz)	1583.7	1565.2	1550.5	1547.9	1.18	0.95	0.17
F-17 (Hz)	2117.1	2090.2	2069.3	2065.1	1.29	1.01	0.20

The second step is to perform EMA on the real singing bowl. In order to obtain real structure's modal parameter, we use the impact hammer to excite the singing bowl in free boundary condition and the accelerometer to pick up the vibration response. Fig. 3(a) shows the experimental setup for performing EMA on the singing bowl, while Fig. 3(b) reveals the 24 measurement points on the ring surface of singing bowl. The accelerometer is fixed at Point 1, and the impact hammer is applied to excite the singing bowl at the 24 grid points. The structural frequency response functions (FRFs), $H_{ai,fj}(f)$ or simply $H_{ij}(f)$, between the acceleration at the i-th location and the impact force at the j-th location can be measured. The 24 sets of FRFs can be imported to the curve-fitting software ME'scopeVES to

determine experimental modal parameters, including natural frequencies, mode shapes and modal damping ratios.

The third step of MV is to compare the obtained modal parameters from FEA and EMA, respectively. The important concept is that if the FE model can be equivalent to the real structure of singing bowl, the numerically obtained and experimentally determined modal parameters should be consistent with each other.

Table 2 summarizes the comparison of natural frequencies obtained from FEA and EMA, respectively. One can observe the axisymmetric modes from FEA, such as modes F-07 and F-08, because of the circular shape of singing bowl. The natural frequencies of two axisymmetric modes are the same from FEA; however, only one mode is obtained from EMA for mode O-01. For modes such as F-11 and F-12, the corresponding experimentally extracted modes are O-03 and O-04, which natural frequencies are not exactly the same. This can be explained that the singing bowl is not in a perfect axisymmetric shape.

For those modes that can be put aside for comparison, the physical meanings of mode shapes should be the same. Table 2 also shows the error percentage of natural frequencies between FEA and EMA. The root mean square (RMS) error for all comparable modes is 4.27%. Only the natural frequency error of the first mode is 7.43%, and other modes are within 5%. This indicates the equivalency of FE model to the real structure of singing bowl.

As one can see in Table 2, the modes can be categorized into two types of modes, including the (z, θ) modes and (r, θ) modes. Those modes are in a reasonable sequence from lower order of modes to higher order, such as (z, θ)=(1,2), (z, θ)=(1,3), and etc.
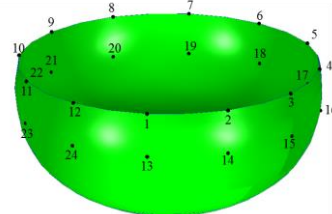
Table 3 shows the theoretical and experimental mode shapes for (z, θ) modes. One can observe both the (z, θ) mode shapes from FEA and EMA agree reasonably to each other. The (z, θ) modes of singing bowl are the ring modes that only the upper ring surfaces will vibrate. For the (z, θ) mode, z is for the vertical direction always with one partition, i.e. z=1, and θ is for the partition number in the circumferential direction.

Table 4 shows theoretical mode shapes for the (r, θ) modes that are the local mode effects due to the bottom surfaces of singing bowl. That the (r, θ) modes are not experimentally measured is the cause of measuring points only on the ring surface as shown in Fig. 3(b). The physical meaning of (r, θ) modes can be characterized for the bottom surface of singing bowl where r is for the radial direction, and θ is for the circumferential direction. It is noted that there is no axisymmetric mode for (r, θ)=(r,0) as shown in Table 2.

Next section will demonstrate that the percussion sound of singing bowl is dominated by the ring modes, i.e. the (z, θ) modes, and the (r, θ) modes related to the bottom surface vibration of singing bowl do not contribute to the sound radiation, because the singing bowl is generally struck at the ring surface.

(a) Instrumentation setup   (b) Grip points for EMA
Fig. 3. Experimental setup for EMA on the singing bowl.

Table 2. Comparison of natural frequencies between FEA and EMA.

FEA			EMA			Natural frequency error (%)
Mode No.	Natural frequency (Hz)	Physical meaning of mode shapes	Mode No.	Natural frequency (Hz)	Physical meaning of mode shapes	
F-07	130.1	$(z,\theta)=(1,2)$	O-01	121.1	$(z,\theta)=(1,2)$	7.43
F-08	130.1					
F-09	363.8	$(z,\theta)=(1,3)$	O-02	361.7	$(z,\theta)=(1,3)$	0.58
F-10	363.8					
F-11	686.3	$(z,\theta)=(1,4)$	O-03	700.0	$(z,\theta)=(1,4)$	-1.96
F-12	686.4		O-04	712.5		-3.66
F-13	1084.8	$(z,\theta)=(1,5)$	O-05	1123.4	$(z,\theta)=(1,5)$	-3.44
F-14	1085.0		O-06	1135.2		-4.42
F-15	1547.9	$(z,\theta)=(1,6)$	O-07	1614.1	$(z,\theta)=(1,6)$	-4.10
F-16	1548.1		O-08	1621.9		-4.55
F-17	2065.1	$(z,\theta)=(1,7)$	O-09	2152.3	$(z,\theta)=(1,7)$	-4.05
F-18	2065.3		O-10	2169.5		-4.80
F-19	2142.8	$(r,\theta)=(1,0)$	-	-	-	-
F-20	2579.3	$(r,\theta)=(1,1)$	-	-	-	-
F-21	2579.3		-	-	-	-
F-22	2627.9	$(z,\theta)=(1,8)$	O-11	2752.3	$(z,\theta)=(1,8)$	-4.52
F-23	2628.0					
F-24	2737.4	$(r,\theta)=(2,0)$	-	-	-	-
F-25	2908.7	$(r,\theta)=(2,1)$	-	-	-	-
F-26	2908.7		-	-	-	-
F-27	3111.7	$(r,\theta)=(1,2)$	-	-	-	-
F-28	3111.7		-	-	-	-
F-29	3205.7	$(r,\theta)=(3,1)$	-	-	-	-
F-30	3205.8		-	-	-	-
F-31	3228.5	$(z,\theta)=(1,9)$	O-12	3357.8	$(z,\theta)=(1,9)$	-3.85
F-32	3228.8		O-13	3382.0		-4.53
F-33	3245.8	$(r,\theta)=(3,0)$	-	-	-	-
F-34	3319.9	$(r,\theta)=(2,2)$	-	-	-	-
F-35	3319.9		-	-	-	-
F-36	3414.9	$(r,\theta)=(1,3)$	-	-	-	-
F-37	3414.9		-	-	-	-
F-38	3486.4	$(r,\theta)=(3,2)$	-	-	-	-
F-39	3486.4		-	-	-	-
F-40	3511.0	$(r,\theta)=(4,0)$	-	-	-	-
RMS for Natural frequency error (%)						4.27

Table 3. Comparison of mode shapes between FEA and EMA for modes (z,θ).
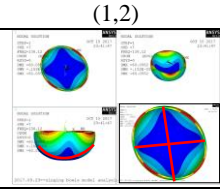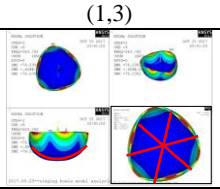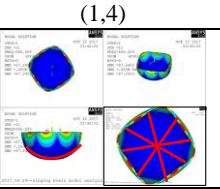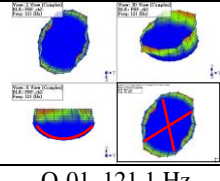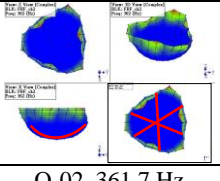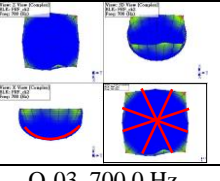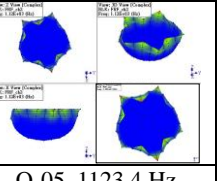
(z,θ)	(1,2)	(1,3)	(1,4)	(1,5)
FEA				
	F-07_130.1 Hz	F-09_363.8 Hz	F-11_686.3 Hz	F-13_1084.8 Hz
EMA				
	O-01_121.1 Hz	O-02_361.7 Hz	O-03_700.0 Hz	O-05_1123.4 Hz

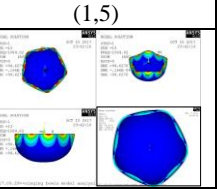**Table 3.** Comparison of mode shapes between FEA and EMA for modes (z, θ) (Continued)

(z, θ)	(1,6)	(1,7)	(1,8)	(1,9)
FEA				
	F-15_1547.9 Hz	F-17_2065.1 Hz	F-22_2627.9 Hz	F-31_3228.5 Hz
EMA				
	O-07_1614.1 Hz	O-09_2152.3 Hz	O-11_2752.3 Hz	O-12_3357.8 Hz

Table 4. Theoretical mode shapes for modes (r, θ) from FEA.

r \ θ	0	1	2	3
1	 F-19_2142.8 Hz $(r,\theta)=(1,0)$	 F-20_2579.3 Hz $(r,\theta)=(1,1)$	 F-27_3111.7 Hz $(r,\theta)=(1,2)$	 F-36_3414.9 Hz $(r,\theta)=(1,3)$
2	 F-24_2737.4 Hz $(r,\theta)=(2,0)$	 F-25_2908.7Hz $(r,\theta)=(2,1)$	 F-34_3319.9 Hz $(r,\theta)=(2,2)$	
3	 F-33_3245.8 Hz $(r,\theta)=(3,0)$	 F-29_3205.7 Hz $(r,\theta)=(3,1)$	 F-38_3486.4Hz $(r,\theta)=(3,2)$	
4	 F-40_3511.0Hz $(r,\theta)=(4,0)$			

3 Correlation of Percussion Sound to Vibration Modes

Section 2 shows the theoretical analysis of vibration modes and experimental verification of FE model for the singing bowl. The structural mode shapes have been physically interpreted for all modes that include the (z, θ) modes and (r, θ) modes. The interest is to know how the vibration modes affect the percussion sound of singing bowl.

The microphone is positioned near the singing bowl away from the edge about 20cm as shown in Fig. 3(a). The singing bowl is stuck by the soft tip stick at the top of ring surface. The time response of sound pressure is measured and performed spectral analysis to obtain the percussion sound spectrum.

Fig. 4 shows the sound spectrum of singing bowl A. On the top of sound spectrum for each peak resonance, the corresponding mode shapes from FEA and EMA are depicted as shown. One can observe that those peak resonances are related to the ring modes, i.e. the (z, θ) modes, and there is no (r, θ) modes in sound spectrum. This is the cause that the (r, θ) modes are not excited for striking on the ring surface.

Since the percussion stick is with a soft tip, the lower modes of vibration can be induced mostly. The sound responses at lower modes are higher, and the sound pressure level become descending at higher modes. The first peak resonance frequency about 118.4Hz can be identified as the fundamental frequency and the rest peak resonance frequencies are the overtones that affect the perceived sound quality.
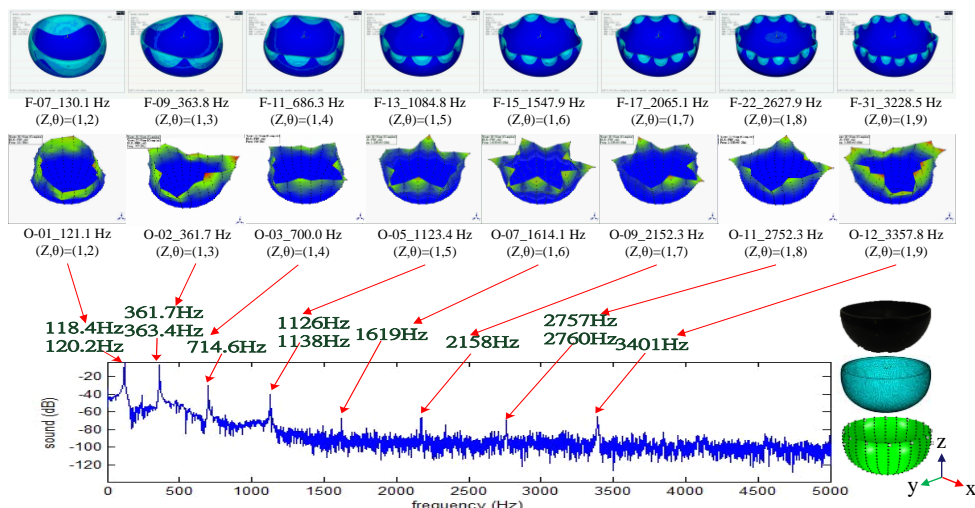

| F-07_130.1 Hz | F-09_363.8 Hz | F-11_686.3 Hz | F-13_1084.8 Hz | F-15_1547.9 Hz | F-17_2065.1 Hz | F-22_2627.9 Hz | F-31_3228.5 Hz |
| (Z,θ)=(1,2) | (Z,θ)=(1,3) | (Z,θ)=(1,4) | (Z,θ)=(1,5) | (Z,θ)=(1,6) | (Z,θ)=(1,7) | (Z,θ)=(1,8) | (Z,θ)=(1,9) |

| O-01_121.1 Hz | O-02_361.7 Hz | O-03_700.0 Hz | O-05_1123.4 Hz | O-07_1614.1 Hz | O-09_2152.3 Hz | O-11_2752.3 Hz | O-12_3357.8 Hz |
| (Z,θ)=(1,2) | (Z,θ)=(1,3) | (Z,θ)=(1,4) | (Z,θ)=(1,5) | (Z,θ)=(1,6) | (Z,θ)=(1,7) | (Z,θ)=(1,8) | (Z,θ)=(1,9) |

Fig. 4. Sound spectrum for singing bowl A.

4 Percussion Sound Characteristics for Different Singing Bowls

Fig. 5 shows the picture of seven different sizes of singing bowls and number from 1 to 7. These singing bowls are designed as a set of bowls. The largest one is Number 1 with the radius of 358mm and the height of 148mm. The interest is how these different sizes of singing bowls sound with the same strike excitation. As we realize the sound generation mechanism for the singing bowl A that is similar to those singing bowls in Fig. 5 in term of geometry characteristics. Therefore, we can examine the sound spectrum and evaluate the sound quality of these singing bowls.

Fig. 5. Different sizes of singing bowls number 1 to 7.

(a) A

(b) 1

(c) 2
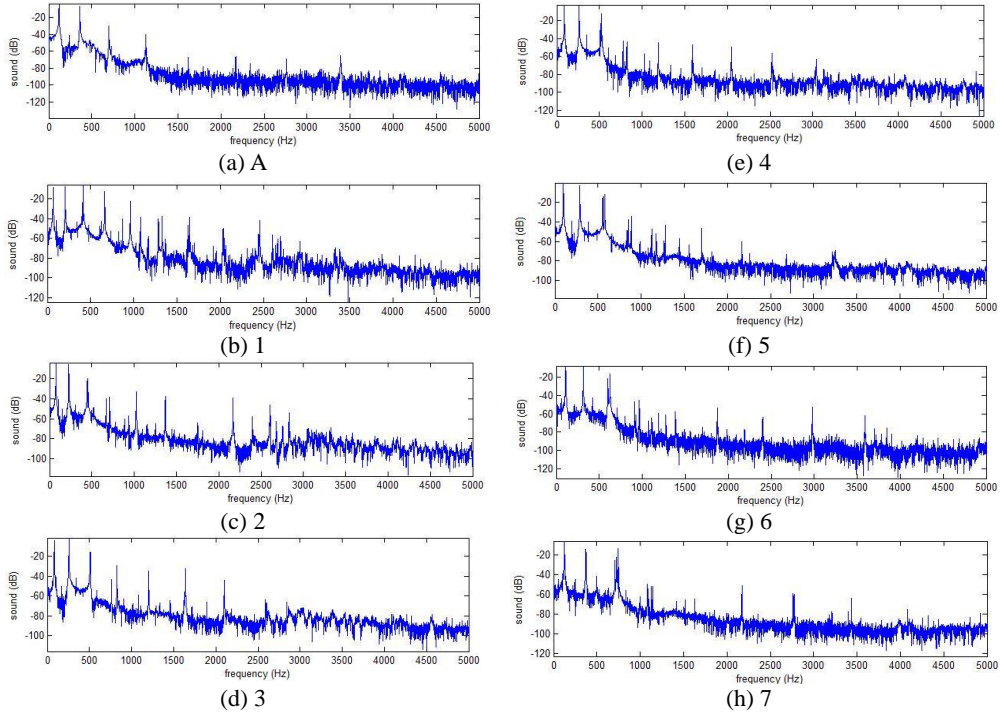
(d) 3

(e) 4

(f) 5

(g) 6

(h) 7

Fig. 6. Sound spectrum of singing bowl A and different sizes of singing bowls number 1 to 7.

The percussion sound measurement is preceded as discussed in Section 3. Sound spectrum for all singing bowls can be obtained and shown in Fig. 6. One can observe that the sound spectrums among these singing bowls are similar to each other; however, the peak response frequencies are different. As discussed, those peak resonance responses come from the structural vibration modes and will reveal the different perceived sound quality.

Table 5 summarizes the peak resonance frequencies from Fig. 6 for singing bowl A and Number 1 to 7. The first peak resonance frequency can be the $(z, \theta)=(1,2)$ mode and known as the fundamental frequency. The higher modes may also contribute to the radiated sound and known as the overtone frequencies. The frequency ratios in Table 4 are obtained by taking the overtone frequencies divided by the fundamental frequency. It is interesting to note that the frequency ratios for all singing bowls appear the values near integer ratios, especially 3 and 6 mostly. The harmonic sound effect is evident, and this is why the perceived sound quality for these singing bowls is felt harmony.

Table 5. Peak resonance frequencies for different singing bowls.

Bowl NO.	A		1		2		3		4		5		6		7	
Mode NO.	Peak Frequency (Hz)	Frequency ratio	Peak Frequency (Hz)	Frequency ratio	Peak Frequency (Hz)	Frequency ratio	Peak Frequency (Hz)	Frequency ratio	Peak Frequency (Hz)	Frequency ratio	Peak Frequency (Hz)	Frequency ratio	Peak Frequency (Hz)	Frequency ratio	Peak Frequency (Hz)	Frequency ratio
S-01	118.4	**1.00**	66.76	**1.00**	75.76	**1.00**	82.14	**1.00**	89.4	**1.00**	99.56	**1.00**	107.4	**1.00**	126	**1.00**
S-02	120.2	1.02	67.63	1.01	225.8	2.98	83.59	1.02	263.3	**2.95**	289.1	2.90	109.1	1.02	128.9	1.02
S-03	361.7	**3.05**	206.1	**3.09**	227.6	**3.00**	256.9	**3.13**	509.1	5.69	290.2	**2.91**	313.2	**3.15**	370.6	2.94
S-04	363.4	3.07	207.8	3.11	441.5	5.83	504.7	6.14	513.5	5.74	555	5.57	596.5	**5.99**	375.3	**2.98**
S-05	714.6	**6.04**	403.4	**6.04**	444.4	5.87	507.9	6.18	526.5	5.89	561.3	5.64	609.8	6.12	710	5.63
S-06	1126	9.51	414.8	6.21	451.6	6.76	513.7	6.25			577.9	5.80	623.7	6.26	722.7	5.74
S-07	1138	9.61	665	**9.96**	454.8	6.81	761.6	9.27			580.5	5.83	626.4	6.29	741.3	5.88
S-08	1619	13.67	960.1	14.38	667	**9.99**	827.5	**10.07**			851.6	8.55			750.3	**5.95**
S-09	2158	18.23	1079	16.16	671.6	10.06	1203	14.65			886.1	8.90				
S-10	2757	23.29	1330	**19.92**	708.2	10.61	1637	19.93								
S-11	2760	23.31			1026	15.37										
S-12	3401	28.73			1369	20.51										
S-13					2169	32.49										

Table 6. Fundamental frequencies for different singing bowls.

Bowl NO.	1	2	3	4	5	6	7
Fundamental Frequency(Hz)	66.76	75.76	82.14	89.4	99.56	107.4	126
Scale	C2	D2	E2	F2	G2	A2	B2
Scale Frequency(Hz)	65.41	73.42	82.41	87.31	98.00	110.00	123.47
Frequency Difference (Hz)	1.35	2.34	-0.27	2.09	1.56	-2.60	2.53
Frequency Error (%)	2.06	3.19	-0.33	2.39	1.59	-2.36	2.05

By examining the fundamental frequencies of the seven singing bowls from 1 to 7, Table 6 summarizes the fundamental frequencies of these singing bowls and compares the fundamental frequencies with musical note's standard frequencies. It is noted that C2-B2 are followed the scientific notation system for pitch notes Do-Si. Note that the frequency differences are within 2 to 3 Hz, and the frequency error is about 2-3%. The set of seven singing bowls is intended for the design to produce musical notes from C, D up to B that is an octave of musical notes.

5 Conclusions

This work conducts theoretical analysis and experimental approach in examining the percussion sound characteristics of a set of singing bowls. A typical singing bowl is first studied to numerically and experimentally determine structural modal parameters. Base on the comparison of natural frequencies and corresponding mode shapes, the FE model of singing bowl can be validated and used to assist on characterize the vibration mode characteristics of singing bowls. The ring modes of singing bowl are the most dominated modes for percussion sound radiation. The local modes at the bottom side of singing bowl can also be identified and do not attribute to generate the percussion sound. The set of seven singing bowls is calibrated to have the fundamental frequencies from C to B of an octave of musical notes. In particular, the harmonic sound effect with the integer frequency ratios of near 3 and 6 is found and revealed a good perceived sound quality.

References

1. B. T. Wang, C. H. Huang, Y. H. Wu, *The 23ⁿᵈ International Congress on Sound and Vibration (ICSV23)*, Paper No.:440 (2016).
2. B. T. Wang, Y. L. Tsai, P. H. Chen, H. Y. Chang, K. T. Yu, *20ᵗʰ International Congress on Sound & Vibration,* Paper No.: 431 (2013).
3. J. Pan, *The Journal of the Acoustical Society of America*, **84**, S1, 135 (2009).
4. J. M. Lee, S. H. Kim, S. J. Lee, J. D. Jeong, H. G. Choi, *Journal of Sound and Vibration*, **257**, 779-790 (2002).
5. N. McLachlan, B. K. Nigjeh, A. Hasell, *The Journal of the Acoustical Society of America*, **114**, 1, 505-511 (2003).
6. N. McLachlan, *75ᵗʰ Acoustical Society of America Conference,* 1-8 (2004).
7. N. H. Fletcher, W. T. McGee, A. Z. Tarnopolsky, *The Journal of the Acoustical Society of America*, **131**, 3, 1437-1444 (2002).
8. A. Myers, R. W. Pyle, J. Gilbert, D. M. Campbell, J. P. Chick, S. Logie, *The Journal of the Acoustical Society of America*, **131**, 678-688 (2012).
9. A. Ezcurra, *Journal of Sound and Vibration*, **194**, 640-644 (1996).
10. R. R. Boullosa, *Applied Acoustics*, **63**, 311-322 (2002).
11. B. T. Wang, Y. C. Lan, C. H. Huang, Y. S. Wu, C. H. Chang, *2013 Annual Meeting and 26th Symposium of Taiwan Acoustical Association*, Paper No.: C5 (2013). (in Chinese)